Electron Spin-Lattice Relaxation at Defect Sites; E' Centers in Synthetic Quartz at 3 Kilo-Oersteds*

J. G. CASTLE, JR., D. W. FELDMAN, AND P. G. KLEMENS
Westinghouse Research Laboratories, Pittsburgh, Pennsylvania

AND

R. A. WEEKS
Oak Ridge National Laboratory,† Oak Ridge, Tennessee

(Received 2 November 1962)

Measurements of the spin-lattice relaxation time T_1 by the inversion-recovery technique are reported for two paramagnetic centers in quartz over a wide temperature range: from 1.3 to 250°K for the E_1' center, and from 2 to 80°K the E_2' center. The data, extending over several orders of magnitude in T_1, are interpreted in terms of cross relaxation, direct processes, and Raman processes. The dominant feature of the Raman relaxation is a temperature variation of about T^3, which is much slower than expected by standard theory.

The theory of spin-lattice relaxation is extended to account for the modification at a defect site of the strain due to a lattice wave. Each defect has at least one characteristic frequency and the local strain due to a wave of higher frequency is enhanced, being essentially given by the displacement due to the wave, rather than its spatial derivative. If the characteristic frequency is sufficiently low compared to the Debye frequency, the Raman relaxation rate should vary as T^3 (or T^5) over a wide range of temperatures, instead of the usual T^7 (or T^9) variation.

A detailed comparison of the relaxation rates observed for the two E' centers with the above theory suggests that each center has two characteristic frequencies or temperatures θ_i. For the E_2' center one of these ($\theta_i=45$°K) is ascribed to the vibration of a neighboring impurity ion, probably a proton. The other temperature ($\simeq 5$°K) may arise from the motion of oxygen ions at the defect. The E_1' center has the two characteristic temperatures of 140°K and 14°K.

A model for the E_1' center is proposed: An electron is trapped at a silicon ion located in an oxygen divacancy. This model leads to the likelihood of low characteristic frequencies through a non-rigid SiO_2 group, and also through a net negative charge, which should attract one or more interstitial impurity ions.

I. INTRODUCTION

ELECTRON spins imbedded in a crystal are relaxed to the lattice temperature by means of lattice vibrations. The main features of the phenomena have been described by Van Vleck[1,2] and Kronig[3] in terms of the normal modes of the perfect lattice. Quantitative predictions were attempted[2,3] for iron group alums and a clear identification was indicated for the direct processes (single phonon emission and absorption) and the Raman processes (inelastic scattering of thermal phonons) by their dependence on temperature and on magnetic field.[4] The temperature dependence of the direct processes has been experimentally verified for several of the iron group ions.[5–10] The temperature dependence of relaxation has been observed for paramagnetic impurity centers in a semiconductor[11] in both the direct and the Raman regions. Tentative assignment of the temperature dependence of the Raman processes has been made for chromium[7,8,12] and for iron.[9,10] Recently Orbach[13] has, with a similar analysis, obtained explicit expressions for the spin-lattice relaxation time due to the direct and the Raman processes in rare earth salts; for the special case of a low-frequency acoustic phonon being resonant with an excited electronic state of the ion, an additional, exponential temperature dependence was indicated. The temperature dependence observed for rare earth ions[14,15] confirms the predictions for the direct, Raman, and resonant Raman processes, at liquid helium temperatures, with the temperature well below the Debye temperature, and the mass of the rare earth ion about equal to the mass of the diluent ion.

Many paramagnetic centers are not imbedded in a perfect crystal but are themselves associated with a defect site. For example, paramagnetic ions dilutely substituted at lattice points usually differ in mass and often differ in net electric charge from the ions they replace. Further,

* Supported in part by the U. S. Air Force through the Air Force Cambridge Research Laboratories.

† Oak Ridge National Laboratory is operated by Union Carbide Corporation for the U. S. Atomic Energy Commission.

[1] J. H. Van Vleck, J. Chem. Phys. **7**, 72 (1939).
[2] J. H. Van Vleck, Phys. Rev. **57**, 426 (1941).
[3] R. L. de Kronig, Physica **6**, 33 (1939).
[4] See also, for explicit calculations involving iron group ions: R. D. Mattuck and M. W. P. Strandberg, Phys. Rev. **119**, 1204 (1960); M. Blume and R. L. Orbach, *ibid.* **127**, 1587 (1962).
[5] J. G. Castle, Jr., P. F. Chester, and P. E. Wagner, Phys. Rev. **119**, 953 (1960).
[6] J. G. Castle, Jr., and D. W. Feldman, Phys. Rev. **121**, 1349 (1961).
[7] A. A. Manenkov and A. M. Prokhorov, Soviet Phys.—JETP **15**, 54 (1962).
[8] J. H. Pace, D. F. Sampson, and J. S. Thorp, Phys. Rev. Letters **4**, 18 (1960); and Proc. Phys. Soc. (London) **77**, 257 (1961).
[9] D. H. Paxman, Proc. Phys. Soc. (London) **78**, 180 (1961).
[10] T. Bray, G. C. Brown, Jr., and A. Kiel, Phys. Rev. **127**, 730 (1962).
[11] G. Feher and E. A. Gere, Phys. Rev. **114**, 1245 (1959); D. K. Wilson and G. Feher, *ibid.* **124**, 1068 (1961); A. Honig and E. Stupp, *ibid.* **117**, 69 (1960).
[12] J. G. Castle, Jr., D. W. Feldman, and P. G. Klemens, *Advances in Quantum Electronics* (Columbia University Press, New York, 1961), p. 414.
[13] R. L. Orbach, Proc. Phys. Soc. (London) **77**, 821 (1961).
[14] C. B. P. Finn, R. L. Orbach, and W. P. Wolf, Proc. Phys. Soc. (London) **77**, 261 (1961); cf., J. A. Cowen and D. E. Kaplan, Phys. Rev. **124**, 1099 (1961).
[15] P. L. Scott and C. D. Jeffries, Phys. Rev. **127**, 32 (1962).

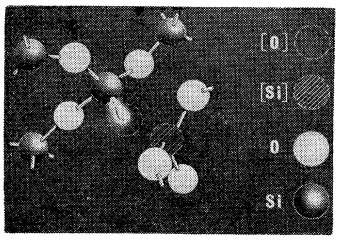

FIG. 1. Proposed structural model for the E_2' center in crystalline quartz. The crystal ball model is shown as viewed about 30° from a [10·0] axis. Regular lattice positions of the silicon and oxygen ions are indicated even though static relaxation around the defect is expected. The locations of the interstitial(s) are not shown.

some paramagnetic centers are located at such defects as vacancies or interstitials. One, therefore, expects the mechanical properties of such defects to alter spin-lattice interactions in their immediate vicinity. A simple modification of the theory of spin-lattice relaxation for defect sites is presented here in which the temperature dependence in the Raman region is markedly changed.

The E' centers in quartz are particularly attractive for studying the Raman relaxation, because they have $S=1/2$ ground states and also large optical splittings. Furthermore, with the open structure of quartz one would expect the mechanical properties of defect sites to differ strongly from those of perfect sites. On the basis of the relaxation data several details are proposed for the models of the E' centers.

The following section summarizes the static characteristics observed for the E' centers in crystalline quartz. A more complete account is given in the companion paper.[16] The theory for spin-lattice interactions at defect sites is outlined in Sec. III. The experimental technique is briefly described and the data are presented in Sec. IV. In later sections, the simplified theory is shown to be a remarkably good description of the relaxation processes, and some model details are discussed.

II. CHARACTERISTICS OF E' CENTERS

The E' centers in crystalline quartz are identified by their magnetic resonance spectra.[16–19] The only optical absorption associated with E' centers occurs near 2200 Å and is spread over some 100 Å but is well resolved[20] from the band gap transition characteristic of quartz.

The ground states of both E_1' and E_2' are Kramers' doublets having a spin of one-half ($S=1/2$), a slight anisotropy in spectroscopic splitting factor ($g=2.00$), and hyperfine structure consistent with the natural abundance and spin of Si^{29}. Each center is an unpaired electron "on" one silicon ion. The magnetic resonance spectra indicate one environment for E_1' centers and several for E_2' centers. While it is apparent that the hyperfine structure obtained[16] from the few centers having Si^{29} at them or near them is the principal source of our understanding of the structure of the centers, this paper will deal with relaxation of those centers having only Si^{28} in and around them and, therefore, having no hyperfine structure due to Si^{29}. These Si^{28} centers give rise to the most prominent resonance lines in the E' microwave spectra.

For interpretation of spin-lattice relaxation the character of the excited electronic states of the E' centers is of interest. Since the structural models for E_1' and E_2' centers are currently being detailed, the excited wave functions are lacking too and it remains for spin-lattice relaxation results to classify the excited states according to whether or not the Van Vleck cancellation controls the Raman processes.[2,13]

A. Production of E' Centers

The E' centers are produced in high-purity silica by Co^{60} γ-ray irradiation.[21] The model proposed[16] for an E_2' center, shown schematically in Fig. 1, is a single electron trapped on a defect silicon ion next to which is a silicon vacancy and from which the nonbridging oxygen ion has been removed during irradiation. For H parallel to [00·1], the three resonance lines are shown in Fig. 2 as observed at 73°K having a g value of about 2.0009. The elements of the g tensor for the central line have not been found separately from the outer pair. The silicon hyperfine structure[16] indicates that there are only three silicon neighbors each probably located beyond each of the three oxygen ions forming bonds to the defect silicon.

The other paramagnetic centers produced by the gamma irradiation have been discussed in some detail elsewhere. Apparently some of the aluminum ions present lose one electron and become paramagnetic. Magnetic resonance lines, similar to those first reported[22] as being due to substitutional Al, appear a few gauss below

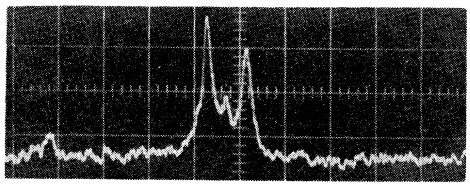

FIG. 2. Resonance absorption by E_2' centers of 9 Gc/sec radiation with the applied field H parallel to the [00·1] axis of sample *CQ*-10 at 73°K. The photograph of the oscilloscope screen shows the three resonance lines for silicon 28 centers with the vertical scale linear in microwave emf and the horizontal scale, linear in magnetic field. The separation of the two large peaks is about 0.4 Oe.

[16] R. A. Weeks, preceding paper [Phys. Rev. **130**, 570 (1963)].
[17] R. A. Weeks, J. Appl. Phys. **27**, 1376 (1956).
[18] R. H. Silsbee, J. Appl. Phys. **32**, 1459 (1961).
[19] R. A. Weeks and C. M. Nelson, J. Am. Ceram. Soc. **43**, 401 (1960).
[20] C. M. Nelson and R. A. Weeks, J. Am. Ceram. Soc. **43**, 399 (1960).
[21] R. A. Weeks and E. Sonder, in *Proceedings of the Conference on Paramagnetism, Jerusalem, Israel, July, 1962* (to be published).
[22] J. H. E. Griffiths, J. Owen, and I. M. Ward, in *Report of the Conference on Defects in Crystalline Solids* (The Physical Society, London, 1955), p. 81.

the E_2' lines shown in Fig. 2. Another center[23] exhibits four equally spaced lines and has $g=2.002$ at H parallel to [00·1].

B. Heat Treatment in Air

The E_2' centers may be removed by bleaching with ultraviolet light at 78°K or by heating above 150°C.[19] On the proposed model this bleaching may take place by the removal of one electron forming a nonparamagnetic E_2 center. Heating to 300°C removes the four-line spectrum and the paramagnetism from the "Al" centers.

E_1' centers are not observed in crystalline quartz after Co^{60} irradiation but are observed after heating to temperatures in excess of 250°C. Upon heating to about 350°C, the E_1' centers disappear.

The concentration of E_2' centers in synthetic crystals after a dose of 10^9R of Co^{60} γ rays is of the order of 10^{16} cm^{-3}. After the heat treatment necessary for the E_1' centers their concentration is of that same order.

C. The E_1' Center

The E_1' centers (with no Si^{29} around) are all equivalent for H parallel [00·1], giving a single line at $g=2.0008$, as shown in Fig. 3. Silsbee has proposed[18] that an E_1' center is a single electron trapped on a silicon. We propose here an improved model based on further microwave data[16] and the relaxation results. We suggest that an E_1' center is a single electron trapped at a silicon ion which is located between two oxygen vacancies; more details are given in Sec. V and the model is shown schematically in Fig. 4. There is presumed to be a collection of one or more interstitial impurity ions around each E_1' center maintaining charge neutrality and contributing to the spin-lattice relaxation.

III. THEORETICAL CONSIDERATIONS

Van Vleck[1,2] has given the theory of the spin-lattice relaxation for an isolated spin in terms of the normal modes of the perfect lattice. We present here an adaptation of that theory for situations where the defect nature of the spin site gives rise to local strains significantly different from those in a perfect lattice. The main features of the usual theory are given and an approximate substitution for the appropriate local strain at a defect site permits the Raman summation to be expressed rather simply in closed form. The resulting expression for the relaxation time is shown to have modified coefficients with the same temperature dependence for the direct term and a markedly different temperature dependence for the Raman terms. Since the present theory is essentially phenomenological, we do not determine separately the values of the effective strain and of the coupling coefficients. However, the temperature dependence is put to experimental test in Sec. V.

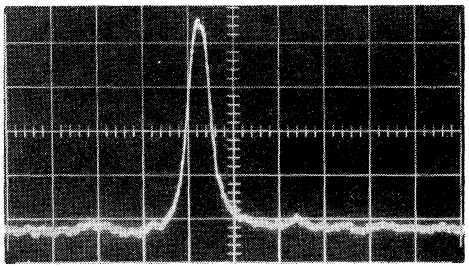

FIG. 3. Resonance absorption of E_1' centers of 9 Gc/sec radiation with the applied field H parallel to the [00·1] axis of sample *GQ*-9 at 4.2°K. The photograph of the oscilloscope screen shows the resonance line for silicon 28 centers with the vertical scale linear in microwave emf and the horizontal scale, linear in magnetic field. The full line width as seen is less than 0.1 Oe.

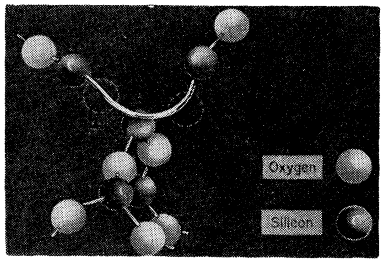

FIG. 4. Proposed structural model for the E_1' center in crystalline quartz. The crystal-ball model is shown as viewed along [10·0]. Regular lattice positions of the silicon and oxygen ions are indicated even though static relaxation of the lattice around the defect is expected. The location(s) of the interstitial is not shown.

A. Relaxation in the Perfect Lattice

The relative spacing of the two spin levels in a magnetic field is perturbed by a change in the crystal field, due to a strain ϵ, and the perturbation Hamiltonian is of the form

$$\mathcal{H}'=A\epsilon+B\epsilon^2, \tag{1}$$

where A and B are the appropriate coupling parameters. The strain ϵ of the arrangement of atoms immediately surrounding the spin site is expressed as the superposition of strains due to the normal modes of the perfect crystal (lattice waves). This perturbation Hamiltonian is substituted into standard second-order perturbation theory, giving the rate of return of the spin population to equilibrium from some nonequilibrium situation. The term $A\epsilon$, which is linear in the phonon field, describes processes in which the spin is reversed with the emission or absorption of a single phonon (direct process), the term $B\epsilon^2$, bilinear in the phonon field, describes two-phonon (Raman) processes.[24]

The strain ϵ at a point $\mathbf{x}$ due to a lattice wave of wave-vector $\mathbf{q}$ in a perfect crystal is given by

$$\epsilon=\frac{1}{G^{1/2}}(\mathbf{p},\mathbf{q})a(\mathbf{q})e^{i(\mathbf{q}\cdot\mathbf{x}+\omega t)}, \tag{2}$$

where G is the number of unit cells in the crystal, $\mathbf{p}$ a unit vector in the polarization direction, $a(\mathbf{q})$ is the dis-

[23] However, this center is not identical with that reported by J. A. Weil and J. H. Anderson, J. Chem. Phys. **35**, 1410 (1961).

[24] See, for example, the phenomenological derivation given by P. G. Klemens, Phys. Rev. **125**, 1795 (1962).

placement amplitude, and $(\mathbf{p},\mathbf{q})$ is either a scalar or vector product, depending on the nature of the strain.

The displacement $a(\mathbf{q})$ is replaced by the oscillator matrix element, i.e.,

$$a(\mathbf{q})=\left(\frac{\hbar}{M\omega}\right)^{1/2}[N \text{ or } (N+1)]^{1/2}, \tag{3}$$

where ω is the angular frequency of the lattice wave, M the atomic mass, N is the number of phonons in the mode considered, and N or $(N+1)$, respectively, is used for the matrix element which describes either the annihilation or the creation of a phonon from the oscillator state of N phonons.

Substituting (2) and (3) into (4), and using only the term $A\epsilon$ as the perturbation, one obtains for the direct-phonon relaxation time

$$\frac{1}{T_{1D}}=32\pi^2\left(\frac{3}{4\pi}\right)^{1/3}\omega_D\frac{A^2(\hbar\omega_0)^2}{Mc^2(k\Theta)^3}\frac{T}{\Theta}, \tag{4}$$

where ω_D is the Debye limiting frequency, Θ the Debye temperature, i.e., $\hbar\omega_D=k\Theta$, c the velocity of sound, and $\hbar\omega_0$, the energy difference between the two spin levels, is assumed to be much less than kT. In deriving (4) one has taken for $(\mathbf{p},\mathbf{q})^2$ the average value $q^2/3$, replaced the equilibrium value of $N(\omega_0)$ by $kT/\hbar\omega_0$, and used the fact that the only phonons which can cause a direct transition are those of frequency ω_0.

In a similar way one expands ϵ^2 in a double sum of lattice waves and derives the Raman relaxation rate.[24] Making the same approximation for $(\mathbf{p},\mathbf{q})^2$ as before, using the equilibrium expression for $N(\omega)$, summing over all pairs of phonons such that $\omega-\omega'=\omega_0$, neglecting ω_0 compared to ω or ω', and taking B independent of ω, one obtains

$$\frac{1}{T_{1R}}=36\pi\left(\frac{B}{Mc^2}\right)^2\omega_D\left(\frac{T}{\Theta}\right)^7 J_6\left(\frac{\Theta}{T}\right). \tag{5}$$

The J factor is given for $n=6$ in the expression

$$J_n(X)=\int_0^X\frac{z^ne^z}{(e^z-1)^2}dz, \tag{6}$$

an integral which is used frequently in transport theory, and which has been tabulated.[25] For Kramers doublets, the Van Vleck cancellation[2,13] can give B to be effectively proportional to the phonon frequency and

$$1/T_{1R}\propto T^9J_8(\Theta/T). \tag{7}$$

We can visualize the effect on T_{1R} due to a modification of the strain by writing (5) in the form

$$\frac{1}{T_{1R}}\propto\int_0^{\Theta/T}\frac{T^7z^6e^z}{(e^z-1)^2}dz. \tag{8}$$

A factor of T^4z^4 arises from the $(\mathbf{p},\mathbf{q})$ factor in the expression (1) for the strain. The remaining factor arises from the thermal average displacements, and the summation over pairs of modes such that $\omega'-\omega=\omega_0$. For the strain at a defect, it is the factor T^4z^4 which must be appropriately modified.

B. Local Strain at a Defect Site

In the usual treatment one uses expression (2) for ϵ in (1), even though (2) holds only in a perfect crystal. In a slightly imperfect crystal Eq. (2) will still hold almost everywhere. However, to calculate T_1 we need the strain in the immediate vicinity of the spin site. When the spin is associated with an impurity or defect, this is precisely where expression (2) fails. We must, therefore, look more closely at the strain at a defect site.

Every defect has associated with it one or more characteristic vibrational frequencies ω_i, which have to be compared to the frequency describing the normal interatomic bond of order ω_D. Roughly speaking, we can expect two classes of behavior: (a) cases when ω_i exceeds ω_D sufficiently, so that the vibrations at that frequency are not propagated through the crystal, but are localized at the defect[26] (The interaction between spins and localized modes has been treated elsewhere.[24]); (b) cases when ω_i falls below ω_D so that localized modes in the usual sense are not formed,[27] but the defect system undergoes forced oscillations[28] under the influence of the lattice waves. We shall be concerned with the latter case here.

To be more specific, consider an interstitial atom in the cage formed by the normal atoms of the crystal which surrounds it. If the normal lattice is at rest, and the interstitial atom slightly displaced from its equilibrium site, it will vibrate about that site with a frequency ω_i. If the lattice is displaced by a lattice wave so that an appropriate average of the displacements of the neighboring atoms is $u=ae^{i\omega t}$, if v is the displacement of the interstitial atom, and if we neglect damping, then the equation of motion of the interstitial becomes

$$d^2v/dt^2=\omega_i^2(u-v). \tag{9}$$

Writing $v=be^{i\omega t}$, it is readily seen that

$$b=a[\omega_i^2/(\omega_i^2-\omega^2)], \tag{10}$$

where a is the same as in (2).

The lattice wave gives rise to two types of deformations about the defect site. If we think of the normal lattice atoms surrounding the interstitial as a "cage," then the shape of this cage is deformed by the lattice

[25] W. M. Rogers and R. L. Powell, *Tables of Transport Integrals*, National Bureau of Standards Circular No. 535 (U. S. Government Printing Office, Washington, D. C., 1958).

[26] E. W. Montroll and R. B. Potts, Phys. Rev. **100**, 525 (1955); see also, H. B. Rosenstock and C. C. Klick, *ibid.* **119**, 1198 (1960).

[27] An effectively localized mode for a case with $\omega_i<\omega_D$ in a Bravais type lattice is discussed recently by R. Brout and W. Visscher, Phys. Rev. Letters **9**, 54 (1962).

[28] A possible example of such forced oscillations at a lattice defect is discussed by H. B. Rosenstock, J. Phys. Chem. Sol. **23**, 659 (1962).

wave. In addition, the interstitial atom will move from its central position in the cage, and the motion relative to the cage is the difference $(v-u)$. Each of these deformations may perturb the spin Hamiltonian independently.

The deformation of the cage, in the absence of the interstitial, would be described by a strain of the usual form (2). Although the interstitial will somewhat modify this deformation, it will not affect the general character of the strain. We shall disregard this modification and use Eq. (2) to describe this strain.

The motion of the interstitial atom relative to the cage leads to a strain of different character, given for negligible damping from Eqs. (9) and (10) by

$$\epsilon' = \frac{v-u}{a_0} = \frac{a}{a_0}\frac{\omega^2}{\omega_i^2-\omega^2}e^{i\omega t}, \tag{11}$$

where a_0 is the appropriate interatomic distance. Clearly, ϵ' is enhanced over ϵ at frequencies near and above ω_i. However, expression (11) cannot be used when summing over the entire frequency range for the Raman relaxation, because the neglect of damping causes Eq. (11) to exaggerate ϵ' when ω is near ω_i.

In order to arrive at a tractable approximation for the Raman relaxation, we divide the phonon spectrum into two parts, $\omega>\omega_i$ and $\omega<\omega_i$, and use for each range the expression derived from (11) for the limiting cases $\omega\gg\omega_i$ and $\omega\ll\omega_i$, respectively. Thus,

$$\epsilon' = (\omega/\omega_i)^2(a/a_0)e^{i\omega t} \quad \text{for} \quad \omega<\omega_i \tag{12}$$

and

$$\epsilon' = -(a/a_0)e^{i\omega t} \quad \text{for} \quad \omega>\omega_i. \tag{13}$$

This crude approximation is, in fact, preferable to the use of expression (11), in which damping was neglected. In the Appendix an exact expression is obtained for the modulus of ϵ' on the assumption of velocity damping. The resulting curve of ϵ'/a as a function of ω is shown in Fig. 5. It is seen that Eqs. (12) and (13) are indeed a reasonable approximation for any effect integrated over the phonon spectrum, for when damping is light, the error, although large, is confined to a narrow band of frequencies, while the error is small everywhere if damping is heavy. In any case, the approximation underestimates the effects due to ϵ'.

C. Relaxation at a Defect Site

We can now regard the spin-lattice relaxation to be effected in two possible ways: The spin may be coupled to the strain ϵ as in Eq. (1), and it may also be coupled to the strain ϵ' (describing the motion of the central atom relative to the center of mass of the cage) through a relation analogous to (1) with coupling parameters A' and B', respectively. The strain ϵ' is also present at a perfect lattice site, but is usually disregarded since it is proportional to the second derivative of the displacement. However, ϵ' is enhanced at a defect site, becoming larger than ϵ for waves of frequency near and above ω_i.

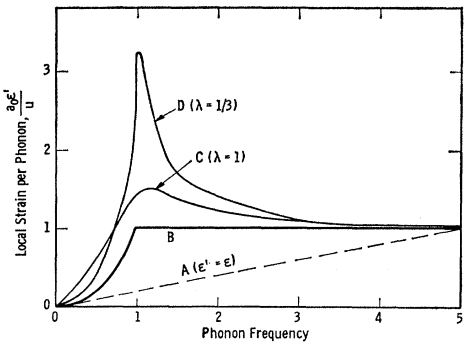

FIG. 5. Dependence of local strain per unit displacement on frequency. The horizontal scale is in units of the characteristic local frequency, ω_i. Curve A represents the usual approximation for the strain modulus in a perfect Debye lattice with $\omega_D=5$; curve B, present approximation; curve C, for velocity-damped harmonic oscillator [Eq. (A3) with $\lambda=1$]; curve D, for velocity-damped harmonic oscillator [Eq. (A3) with $\lambda=1/3$]. The present approximation underestimates the local strain at all frequencies as indicated by the excess of curves C and D over curve B.

The question arises whether the coupling coefficients A' and B' for the odd modes are zero. For a spin site of high symmetry A' would indeed be zero,[1] but if the symmetry is sufficiently low it may not vanish. The term in B' arises from two causes: (1) the term $A'\epsilon'$ taken to second order, (2) and a contribution due to the essential nonlinearity of the effect of strain on the electronic states. The first contribution vanishes if A' vanishes, but there is no symmetry requirement that would make the second contribution vanish. Thus, in general, B' does not vanish and the odd modes contribute to the Raman relaxation, even if they should not contribute to the direct relaxation.

The direct relaxation is still given by Eq. (4), except that A^2 is now replaced by

$$A^2 \rightarrow A^2+\alpha(A')^2(\omega_0\omega_D/\omega_i^2), \tag{14}$$

where α is a numerical factor. Since there is an arbitrariness in our definition of ϵ', there is a corresponding arbitrariness in A' and thus in α. If we take a_0^3 to be the volume per atom of the normal crystal, $\alpha=(4\pi/3)^{2/3}(2\pi)^{-2}$. We have assumed that $\omega_0<\omega_i$, and unless ω_i is very small compared to ω_D, the second term of Eq. (14) can be neglected.[29] In any case, this would affect not the temperature dependence, but only the magnetic field dependence of the direct process.

The contribution of $B'(\epsilon')^2$ to the Raman relaxation can be calculated analogously to (5), using Eqs. (12) and (13) for ϵ'. Note now that the term in $(B')^2$ can be derived from (5) simply by considering the different

[29] In the unusual case of $\omega_i\ll\omega_0$, the additional term would be $\alpha(A')^2(\omega_D/\omega_i)^2$ and this contribution to $1/T_{1D}$ would be independent of ω_0 and thus independent of the magnetic field. The case $\omega_i\rightarrow 0$, which is a special case of our theory, has been treated by A. B. Roitsin, Fiz. Tverd. Tela **3**, 2879 (1961).

dependence of ϵ' on phonon frequencies: The contribution from frequencies $\omega>\omega_i$ is enhanced by a factor

$$(\epsilon'/\epsilon)^4=\alpha^2(\omega_D/\omega)^4 \quad (\text{for all } \omega>\omega_i), \tag{15}$$

while the contribution from frequencies $\omega<\omega_i$ is reduced by

$$(\epsilon'/\epsilon)^4=\alpha^2(\omega\omega_D/\omega_i^2)^4 \quad (\text{for all } \omega<\omega_i). \tag{16}$$

Thus, we obtain for the Raman relaxation rate

$$\frac{1}{T_{1R}}=\frac{36\pi}{M^2c^4}\omega_D\left\{B^2\left(\frac{T}{\Theta}\right)^7 J_6\left(\frac{\Theta}{T}\right)\right.$$
$$+\alpha^2(B')^2\left[\left(\frac{T}{\Theta}\right)^3 J_2\left(\frac{\Theta}{T}\right)-\left(\frac{T}{\Theta}\right)^3 J_2\left(\frac{\Theta_i}{T}\right)\right.$$
$$\left.\left.+\frac{T^{11}}{\Theta_i^8\Theta^3}J_{10}\left(\frac{\Theta_i}{T}\right)\right]\right\}, \tag{17}$$

where $\Theta_i=\hbar\omega_i/k$. It is easily seen that the fourth term in Eq. (17) is always less than the third. Note that Eq. (17) contains a gross simplification due to the use of Eqs. (12) and (13).

We must now distinguish further between two cases: (1) when ω_i is not very much below ω_D, and (2) when ω_i is substantially below ω_D. An example of the first case is Cr(+3) in MgO, discussed earlier.[12] Because the chromium ion is heavier than the magnesium ion it displaces, the defect may have a characteristic frequency of the order $\omega_i=m^{-1/2}\omega_D$, where m is the ratio of the masses of chromium and magnesium. For lattice waves of higher frequency, the local strain would then be enhanced, and the spin-lattice relaxation time vary *more* rapidly than one would expect according to (5) at temperatures well below Θ_i.

We shall be concerned here with the second case, when Θ_i is well below Θ, so that there is a wide temperature range for which $\Theta_i<T<\Theta$. The relaxation will then arise mainly from modes of frequency $\omega>\omega_i$, for which ϵ' is enhanced. The temperature variation of $1/T_{1R}$ is then essentially T^3 over a wide range of temperatures, for the dominant term in Eq. (17) is the second one, proportional to

$$(T/\Theta)^3 J_2(\Theta/T). \tag{18}$$

The "ordinary" Raman relaxation, being reduced by a factor of order $(T/\Theta)^4$, is then expected to be small unless B is very much larger than B'.

At temperatures below Θ_i, the other terms in (17) will gradually gain in importance. For T below about $\Theta_i/6$, $1/T_{1R}$ will vary essentially as $\exp(-\Theta_i/T)$ due to the contribution from modes $\omega>\omega_i$. Furthermore, one expects direct processes and cross relaxation to become important at sufficiently low temperatures.

There is the possibility of defect Raman relaxation occurring for a Kramers doublet whose normal Raman terms have the form $T^9 J_8(\Theta/T)$. In those cases one would expect an expression analogous to (17) of the form

$$\frac{1}{T_{1R}}\propto\left(\frac{T}{\Theta}\right)^9 J_8\left(\frac{\Theta}{T}\right)+C\left[\left(\frac{T}{\Theta}\right)^5 J_4\left(\frac{\Theta}{T}\right)\right.$$
$$\left.-\left(\frac{T}{\Theta}\right)^5 J_4\left(\frac{\Theta_i}{T}\right)+\frac{T^{13}}{\Theta_i^8\Theta^5}J_{12}\left(\frac{\Theta}{T}\right)\right]. \tag{19}$$

Although we have so far considered only one special case explicitly, namely, an impurity atom carrying the spin, surrounded by a cage of normal atoms, the same considerations apply more generally. For example, it is possible to have the spin at an atom which is firmly bound to the lattice, but has a neighboring cell which contains a loosely bound interstitial. This interstitial may generate an electric field at the spin site, and its motion can then contribute to the relaxation. Here the out-of-phase vibration of the interstitial would again lead to an enhanced interaction, and though the parameter B' may be somewhat smaller, the general behavior would again be similar.

Again, it is possible to have a complex defect with internal vibrational degrees of freedom, some of which may have a low characteristic frequency. Such an internal vibrational mode need not be coupled to all lattice displacements—it may be preferentially coupled to lattice waves of some particular polarization. The details of this coupling will effect the magnitude of the corresponding interaction, but not its temperature dependence. The Raman relaxation rate may, thus, be additively composed of several terms, e.g., one of the form of Eq. (5), and others of the form (17).

IV. EXPERIMENT

A. Technique

The spin-relaxation time τ was measured by monitoring the recovery of thermal equilibrium following inversion of the spin magnetic moment by adiabatic rapid passage.[30] All measurements were made at approximately 9.2 kMc/sec, and therefore, near 3000 Oe. Pulsed field sweep was used both for inversion and for monitoring the resonance by a sensitive superheterodyne spectrometer with cathode-ray oscilloscope output.[5] For $\tau\lesssim 2$ sec, the cyclic method previously described[5] was used. For longer times, which were encountered at low temperatures, the method was modified in that the recovery of the E' line from a single inversion was observed a number of times over several time constants by occasionally sweeping the resonance through the observing frequency.

The field sweep of many line widths was obtained by applying a trapezoidal current pulse to a pair of Helm-

[30] An excellent description is given by A. Abragam, *Principles of Nuclear Magnetism* (Oxford University Press, New York, 1961).

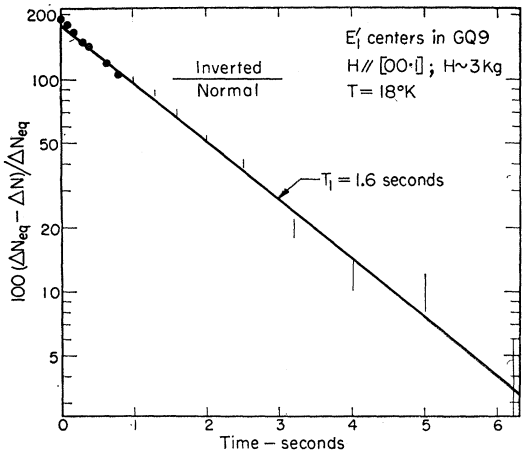

FIG. 6. Recovery of thermal equilibrium of E_1' centers in GQ-9 at 18°K. The vertical scale is the logarithm of the fractional deviation from equilibrium spin populations and the horizontal scale, real time delay after inversion. The points are interpreted in terms of the best fit for a straight line (as shown) whose slope gives the relaxation time, T_1, to $\pm 10\%$.

holtz coils mounted on the reflection cavity[31] containing the sample. In order to avoid broadening the observed line, it is necessary that a good Helmholtz geometry be employed. For example, a sweep of 100 line widths (or 10 Oe) gave no more than 20% broadening in sample GQ-9 which measured 1 cm along eight edges. The peak signal voltage, corrected for instrumental nonlinearities, seen on each sweep was taken to be proportional to the difference in the spin populations. This assumption is valid where there is no change in the line shape during recovery. The inspection of the complete line by field sweep allows direct confirmation of this assumption for each reading.

The relaxation time was measured by plotting the logarithm of the deviation from equilibrium versus time after inversion. When these points yield a straight line, its slope is taken to be τ. A typical plot is shown in Fig. 6 from which τ was determined to $\pm 10\%$.

The power input to the resonant cavity was kept low enough to avoid observable saturation effects. 10^{-8} W with a dwell time of ~ 20 μsec was found to be low enough to meet this criterion.

The cavity coupling was adjusted to the desired reflection coefficient for each temperature by a remotely controlled sliding-vane tuner[32] located just above the cavity. Each sample (with a copper-constantan thermocouple attached to it) was mounted in the microwave cavity so that liquid helium could circulate past its surfaces. The thermocouple was used to indicate the sample temperature above the liquid helium range.[33] Runs made with liquid neon indicated the thermocouple calibration was accurate to $\pm$ one microvolt, when referred to the helium reading.

The measured relaxation time τ for a particular exponential recovery of a dilute spin system may be the result of a sum of independent relaxation processes each characteristic of the isolated spin center. The usual collection of mechanisms include: cross relaxation[34,35] (by spin coupling to spins outside of the line being observed), and the spin-lattice processes—one or more direct processes and one or more Raman processes. The expression for τ is, then,

$$\frac{1}{\tau}=\frac{1}{\tau_c}+\frac{1}{T_{1D}}+\frac{1}{T_{1R}}, \tag{20}$$

where the relative values of the three terms are evaluated experimentally by the dependence of τ on temperature, and on magnetic field orientation and strength.

For $S=1/2$ spins, such as the E' centers, the curvature of a recovery in which the line shape does not change is sufficient evidence for cross relaxation. The deviation from a single exponential indicates the other spin system is warming up as the $S=1/2$ system is cooling down. The reverse unfortunately does not hold and a single exponential may be due to cross relaxation where the other spin system remains at the lattice temperature.

There may be a variety of conditions in which the $S=1/2$ line shape changes during recovery. One of these is a deliberate "hole" used to determine the degree of inhomogeneity in the resonance line. A changing line shape reveals spin-spin interactions within the $S=1/2$ system, and therefore, cannot affect the spin-lattice relaxation except when the $S=1/2$ system is itself composed of different sets of spins having several classes of spin-lattice interactions.

B. Samples

The samples were prepared by bombarding polished crystals of synthetic quartz in a Co^{60} source at Oak Ridge National Laboratory and by a subsequent heating in air. Some details are given in the companion paper. Sample dimensions were roughly $1\times1\times0.2$ cm^3.

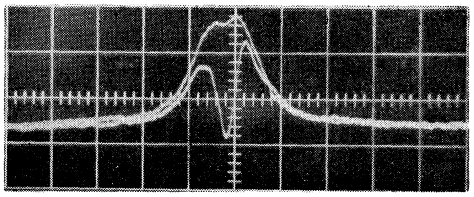

FIG. 7. Holes in the resonance line of E_1' centers in GQ-9 at 27.3°K. The delay times for the two traces are 0.10 and 1.70 sec. The complete line was observed to have $T_1=0.44$ sec at this temperature.

[31] P. F. Chester, J. G. Castle, Jr., P. E. Wagner, and G. Conn, Rev. Sci. Instr. **30**, 1127 (1959).

[32] B. R. McAvoy, Rev. Sci. Instr. **33**, 129 (1962).

[33] A careful calibration of this thermocouple vs a calibrated platinum resistance thermometer gave excellent agreement (± 1 μv on the emf for ΔT from 4.2) with the published tables of the National Bureau of Standards; R. L. Powell, M. D. Bunch, and R. J. Corruccini, Cryogenics **1**, 139 (1961).

[34] N. Bloembergen, S. Shapiro, P. S. Pershan, and J. O. Artman, Phys. Rev. **114**, 445 (1959).

[35] A. Kiel, Phys. Rev. **120**, 137 (1960); **123**, 2202(E) (1961).

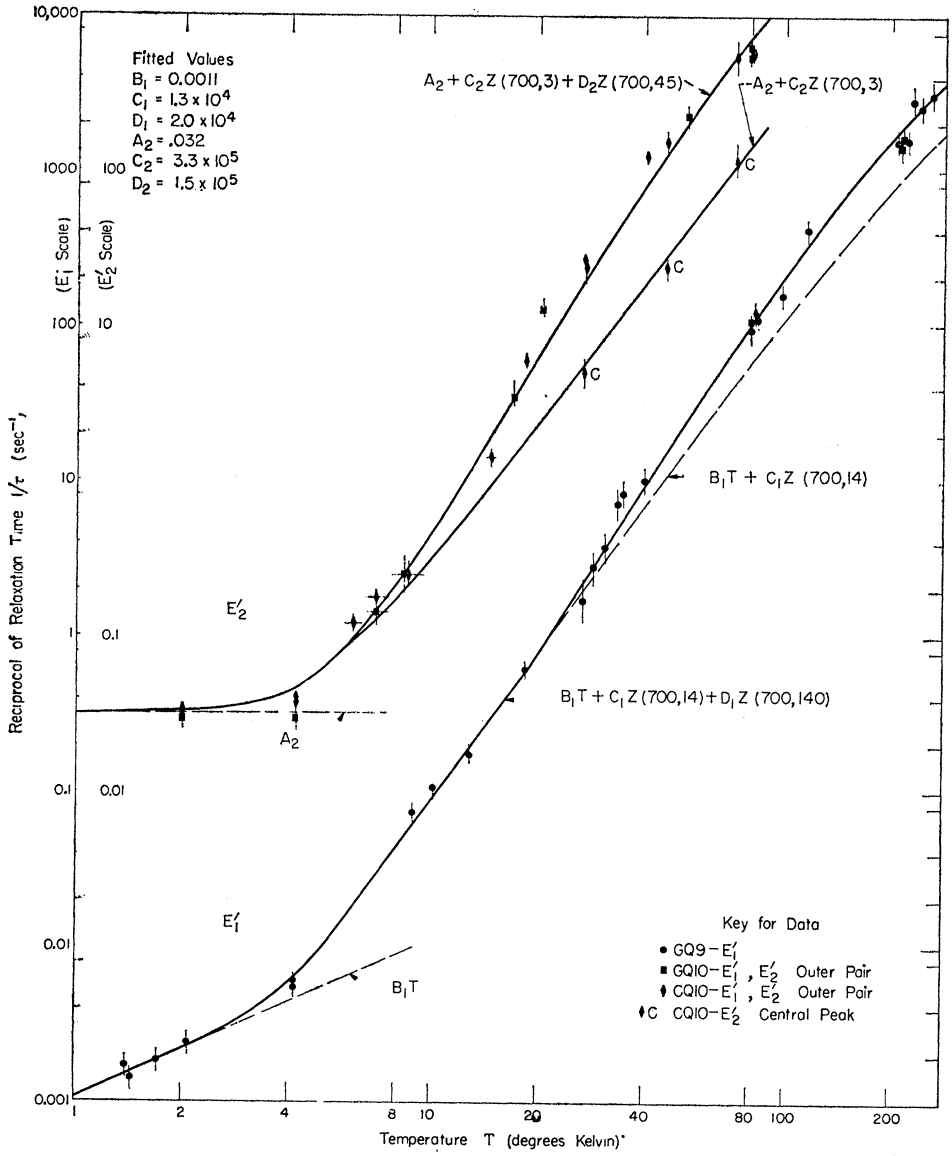

FIG. 8. Reciprocal of observed relaxation time constant for E_1' and E_2' centers in synthetic quartz *vs* lattice temperature. Points marked *C* refer to central line of E_2' resonance, shown in Fig. 2 (see text). The magnetic field of 3000 Oe was applied parallel to [00.1].

Relaxation data were taken on three samples *GQ*-9, *GQ*-10, and *GQ*-12, cut from the same mother crystal[36] grown on a *Z*-cut seed and one sample, *CQ*-10, from another crystal[37] grown on a *Y*-cut seed. Analysis[38] indicated the impurity densities of the *GQ* crystal (atom ratio to Si) to be approximately: Na—200 ppm, Al—100 ppm, Ca—50 ppm, Cu—10 ppm, and Fe—10 ppm; the *CQ* crystal had the same principal impurities with less aluminum by a factor of 5. After irradiation near room temperature the densities of paramagnetic Al centers were about 10 ppm, of the four-line centers about 1 ppm, and after heating to about 300°C there were no paramagnetic Al centers.

[36] Grown by General Electric Ltd., England, and kindly supplied by C. S. Brown.

[37] Grown by Clevite Research Corporation, Cleveland, Ohio, and kindly supplied by D. Hale.

[38] The flame spectroscopy was performed by the spectroscopy group at ORNL.

C. Results for E_1' Centers

Figure 3 shows the appearance of the E_1' resonance for sample *GQ*-9 at $T=4.2$°K and $H\approx3200$ Oe. The magnetic field is parallel to the *c* axis. The central line is due to centers having no hyperfine interaction with Si^{29}, and all measurements of E_1' relaxation were made on this line. The spin concentration was measured to be 2 ppm.[16] The half-power line width is ≈60 mOe and the line is inhomogeneously broadened at least on the time scale of the τ measured for the complete line at 27°K. The inhomogeneity is shown by inverting only a section of the line. The "hole" which is, thus, produced dis-

appears with a time constant[39] approximately equal to τ. The appearance of a typical hole is shown in Fig. 7 at two different delay times.

Figure 8 shows the reciprocal relaxation time $(1/\tau)$ for E_1' as a function of temperature between 1.2 and 250°K for several samples. Each point represents the slope of an exponential recovery curve such as is shown in Fig. 6. The vertical spread indicated for each point was determined by the scatter in the recovery curve, with the usual minimum spread of $\pm 10\%$ being assigned because the recovery curves were not often taken over more than one decade. Uncertainty in the lattice temperature was appreciable only in the range just above 4.2°K. The solid curve in Fig. 6 is given by

$$\frac{1}{\tau}=A_1+B_1T+C_1\left(\frac{T}{\Theta_D}\right)^3\left[J_2\left(\frac{\Theta_D}{T}\right)-J_2\left(\frac{\Theta_1}{T}\right)\right]+D_1\left(\frac{T}{\Theta_D}\right)^3\left[J_2\left(\frac{\Theta_D}{T}\right)-J_2\left(\frac{\Theta_1'}{T}\right)\right], \quad (21)$$

with $A_1=0$, $B_1=0.0011$ sec^{-1} deg^{-1}, $C_1=1.3\times10^4$ sec^{-1}, $D_1=2.0\times10^4$ sec^{-1}, $\Theta_1=14$°K, and $\Theta_1'=140$°K. These parameters were empirically chosen to give the best fit with $\Theta_D=700$°K. Curves of the form $(T/\Theta_D)^7J_6(\Theta_D/T)$ and $(T/\Theta_D)^5J_4(\Theta_D/T)$ are much too steep even with a Debye temperature of 300°K.

Measurements with $H\perp c$ indicate that τ is independent of angle for E_1' at 2.1 and at 80°K.

D. Results for E_2' Centers

Figure 2 shows the appearance of the E_2' resonance in sample CQ-10 at $T=79$°K. The two outer peaks are somewhat broader at 4.2°K as shown in Fig. 9. Here the central peak is barely discernible. The spin concentration was measured to be about 1 ppm,[16] the half power line width of each of the outer peaks was about 60 mOe at $T=79$°K. The resonance line is inhomogeneously broadened to the extent that a "hole" inverted anywhere in the lines recovered with a time constant equal to that of the whole line ($\approx$30 sec at 4.2°K). Figure 8 shows the reciprocal relaxation time for E_2' in several samples from 2 to 80°K. Above 15°K τ was found to be longer for the central peak than for the outer peaks. The relaxation time for the central peak is indicated by the letter C adjacent to each point. The upper solid curve is of the form

$$\frac{1}{\tau}=A_2+B_2T+C_2\left(\frac{T}{\Theta_D}\right)^3\left[J_2\left(\frac{\Theta_D}{T}\right)-J_2\left(\frac{\Theta_2}{T}\right)\right]+D_2\left(\frac{T}{\Theta_D}\right)^3\left[J_2\left(\frac{\Theta_D}{T}\right)-J_2\left(\frac{\Theta_2'}{T}\right)\right], \quad (22)$$

with $A_2=0.032$ sec^{-1}, $B_2=0$, $C_2=3.3(10^5)$, $D_2=1.5(10^5)$, $\Theta_2=3$°K, and $\Theta_2'=45$°K. The constants Θ_2 and C_2 were chosen to fit the relaxation rate for the central peak. The constants D_2 and Θ_2' were then chosen to fit the data of the major lines above 20°K.

At helium temperatures τ for E_2' was found to depend on the field direction but not at 80°K. In fact, the angular dependence of T_1 for E_2' together with the range of T_1's found in the four-line spectrum clearly indicate the dominance of cross relaxation to the aluminum centers at and below 4.2°K.

V. DISCUSSION OF E_1' CENTER

A. Inhomogeneity of Resonance Line

Since the time for a "hole" inverted in any portion of the resonance line for the crystal with about 1 ppm of E_1' centers takes seconds to "heal" or disappear into a normal line shape, the line is obviously inhomogeneous. This is in agreement with the observed line width of some 60 to 100 mOe being much wider than the homogeneous dipolar width estimated by the Van Vleck-Kittel-Abrahams method.[40] We are not sure how much of the observed inhomogeneity is spatial variation in the applied static field; we are sure that less than 20% of it arises from the field of the sweep coils even when we were sweeping a hundred line widths. It remains for more refined measurements to relate the inhomogeneity of E_1' resonance lines to possible sources of line broadening such as distant hyperfine coupling, spatial variation of crystal orientation, or aggregated crystalline imperfections.

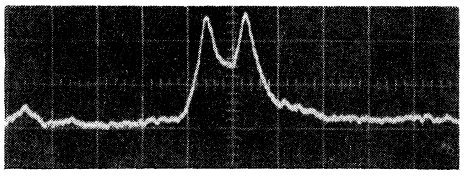

FIG. 9. Resonance absorption of E_2' centers in CQ-10 at 4.2°K. Conditions are identical to those for Fig. 2 except for the temperature. The separate resonances are considerably broader.

B. Absolute Value of T_1

The absolute value of T_1 at 3000 Oe for E_1' centers in synthetic quartz at any temperature above 4°K is specified by our measurements to an accuracy of $\pm 10\%$ according to the agreement shown in Fig. 8. No differences in relaxation were observed between the two series of samples. The samples were quite dilute. Finally, they had impurity concentrations reasonably typical of synthetic crystals of quartz.

[39] For a discussion of spectral diffusion within a resonance line, see for example: W. B. Mims, K. Nassau, and J. D. McGee, Phys. Rev. **123**, 2059 (1961); A. Kiel, *ibid.* **125**, 1451 (1962).

[40] J. H. Van Vleck, Phys. Rev. **74**, 1168 (1948); C. Kittel and E. Abrahams, *ibid.* **90**, 238 (1953).

Therefore, we conclude that the values observed are characteristic of isolated E_1' centers in synthetic crystalline quartz to an accuracy of better than $\pm 20\%$.

In the liquid helium range the T_1 values for E_1' centers in *GQ*-9 are accurate relative to each other to about 10%; the principal source of uncertainty in observing such long T_1's is the stability of the normal absorption signal (at infinite time after inversion) for such narrow lines. One other source of error was a speeding up of recovery due to cross relaxation to the wings of the E_1' line when the magnetic field for recovery, H_R, was much less than 1 Oe from the resonant field H_0; this error in T_1 was made negligible by sweeping so that $H_0-H_R\approx 5$ Oe during recovery.

In the liquid helium range the T_1 values for 3000 Oe agree between samples to better than 20%. The size of the cross-relaxation term may, however, be somewhat larger than 20% of the observed τ.

C. Temperature Dependence from 1.2 to 4.2°K

The T_1 values for E_1' in *GQ*-9 from 1.2 to 4.2°K, shown in the lower left portion of Fig. 8, are interpreted as being due solely to direct processes, as indicated by the term $B_1T=0.0011T$ sec^{-1} and $A_1=0$. Therefore, we conclude that the sum of the Raman terms at 4.2° is no more than 0.001 sec^{-1} and, on this basis, the "critical frequency" associated with the Raman term is no less than $(10/700)\omega_D$, and not as large as $(22/700)\omega_D$ for the E_1' center.

An alternate explanation is possible because of the similarity of the sum $A_1+C_1T^3$ with the linear term B_1T. Presumably a finite rate of cross relaxation is to be associated with the "oxygen" centers. As the cross relaxation through A in the expression for $1/\tau$ is increased from zero, the lower limit on the critical frequency goes down below $(10/700)\omega_D$. A test of the blend of $A+BT$ and CT^3 is planned at 12 000 Oe and investigation of a more varied series of samples is underway.

D. Temperature Dependence above 4.2°K

Raman relaxation via a loosely coupled acoustic response at or near the isolated spin center should, according to the present theory [Sec. III, Eq. (17)], show a temperature dependence of the form $Z(\Theta_D,\Theta_i)=(T/\Theta_D)^3[J_2(\Theta_D/T)-J_2(\Theta_i/T)]$. The T_1 values found for E_1' centers can be fitted to within about 20% over the range of six orders of magnitude by the sum of two such functions; the values are given in Sec. IV and on Fig. 8. The fit is essentially unique on the following bases: The only five theoretical expressions available for Raman relaxation of a spin center which is clearly a $S=1/2$ Kramers doublet are: $(T/\Theta)^9J_8(\Theta/T)$; $(T/\Theta)^7J_6(\Theta/T)$; the corresponding functions for cases of enhanced local strain, $(T/\Theta)^5[J_4(\Theta/T)-J_4(\Theta_i/T)]$ and $(T/\Theta)^3[J_2(\Theta/T)-J_2(\Theta_i/T)]$; and an exponential of the form $\exp(-\Delta/kT)$, where Δ corresponds to a well-defined energy gap in the spectrum of the lattice or of the ion. There are constraints on the Θ's, namely, (1) Θ in $J_2(\Theta/T)$ should equal the Θ_D determined by specific-heat measurements, (2) Θ in J_8 and J_6 may differ somewhat from the specific heat value. According to the anisotropy observed in the acoustic velocity,[41] the Θ in J_8 or J_6 might be as low as $0.7\Theta_D$, (3) Θ in J_4 may be intermediate between (1) and (2) but must be very closely Θ_D, (4) Θ_i is less than Θ in J_2 and J_4. Now the expressions next closest to the T^3 one, namely, the T^5 one with $\Theta=\Theta_D$ or the T^7J_6 with $\Theta=\frac{1}{2}\Theta_D$, are several orders of magnitude too low at the low-temperature end. Therefore, the two T^3 functions given are the best fit of the Raman relaxation for E_1'.

One conclusion from the T^3 dependence is that crystal field splitting, say δ, between the excited states of the E_1' center is small enough to allow strong mixing of the excited states by the applied field of 3000 Oe. The discussion of this general case by Orbach[13] indicates the T^9J_8 and T^7J_6 terms can exist when $\mu H/\delta\approx kT/\Delta$ and that the latter will dominate for $\mu H/\delta\gg kT/\Delta$. The excited states for E_1' are 2100 Å up and so $\Delta/k\cong 70\,000$°K. One is tempted, therefore, to use a sum of

$$T^5[J_4(\Theta_D/T)-J_4(\Theta_i/T)]+T^3[J_2(\Theta_D/T)-J_2(\Theta_j/T)]$$

to fit the data in Fig. 8. The fit is not as good as with the two T^3 functions indicated in Fig. 8, but addition of some resonant strain would probably make such a fit to the data acceptable. The argument for the T^3 rests on the wide range of temperatures over which the function must agree with the data in Fig. 8. The conclusion will be checked by similar T_1 measurements at 12 kOe.

E. Crystalline Model for E_1'

During the course of this study, the model for an isolated E_1' center has been extended. The structural features of the proposed E_1' model are indicated schematically in Fig. 4. We suggest that an E_1' center consists of either one electron or three electrons trapped on the silicon located between the two oxygen vacancies. There may be one or more interstitial (alkali or alkaline earth) ions trapped nearby. Since no hyperfine structure to a sodium nucleus is observed[16] any such interstitial must be an alkaline earth or must be located reasonably far from the defect silicon. The hyperfine couplings for Si^{29} are compared in the companion paper with those of the E_2' center and with those of the similar defect centers in crystalline silicon.[42]

The proposed model for E_1' offers several sources of low-frequency vibration and loose coupling which could give rise to the observed Raman relaxation. One source is apparently (from Fig. 4) the vibrations of the com-

[41] Values of the velocity measured for several angles were kindly made available to us by J. de Klerk and D. I. Bolef.

[42] G. D. Watkins and J. W. Corbett, Discussions Faraday Soc. **31**, 86 (1961).

pound pendulum of SiO_2 along the direction between the oxygen vacancies. Another possible source is the vibrations of each of the two SiO_3 complexes located outside of the divacancy. Another could be an interstitial located in the open c channel of the quartz lattice. Assignment of the two characteristic frequencies (Fig. 8) to specific sources cannot be made with the available data.

VI. DISCUSSION OF E_2' CENTERS

E_2' centers are distinguished from E_1' centers by their response to heat treatment and by the details of their microwave spectra, their optical spectra, and their relaxation. The general similarity of the spectra of E_2' and E_1' centers is discussed in the companion paper. The general similarity in their Raman relaxation is obvious from Fig. 8.

A. Absolute Value of T_1

The agreement between different samples observed for T_1 at 80°K leads us to conclude the values of relaxation time given in Fig. 8 are characteristic of the isolated E_2' center in synthetic crystalline quartz. Specifically, T_1 in the Raman region for the outer pair of lines is characteristic of E_2' centers with an impurity configuration which includes a proton and T_{1R} for the central peak is for E_2' centers with a similar configuration but without the proton. The accuracy in the Raman region is apparently better than $\pm 20\%$.

The 30-sec relaxation time observed to be independent of T between 2.1 and 4.2°K (and surprisingly similar between samples) has been unambiguously identified as arising from cross relaxation to the aluminum centers. The Al centers were, in turn, observed to have a $T_1=0.10$ sec at 2.1°K which is short enough to meet the requirement that the "other" spin system remain at the lattice temperature in order to produce exponential recoveries.

B. Raman Relaxation

The small central line of the E_2' spectrum shows Raman relaxation which can be fitted by a single defect Raman function with $7°K > \Theta_i > 1°K$ and $\Theta_D = 700°K$. This relaxation time is T_{1R} for an E_2' center without a proton trapped adjacent to it. The two larger peaks have faster relaxation than the central one, except below 14°K where their relaxation is observed to be identical. We conclude that there is an extra relaxation mechanism for the two larger lines, probably associated with a loosely bound proton. The observed temperature dependence of the breadth of the outer two lines is consistent with thermal activation of a 45°K motion of an impurity ion which is one source of inhomogeneous line broadening as well as the source of the extra relaxation mechanism.

Assignment of the observed characteristic frequencies (Fig. 8) to a source of loose coupling or local vibration is, therefore, unique. The characteristic temperature of 45°K exists in the motion of an impurity ion trapped adjacent to the E_2' center. This ion is the proton or some other impurity associated with the proton. The characteristic temperature between 7 and 1°K exists either in the motion of the central silicon ion relative to the three oxygens bonded to it or in the motion of the three oxygens beyond the silicon vacancy. In either case, a very low frequency seems reasonable; the former has some similarity to inversion in NH_3 for example.

Again the use of a T^3 function to fit the data in the Raman region implies a mixed character[13] to the excited state of an E_2' center which would have given $(1/T_{1R}) \propto H^2 T^7 J_6(\Theta/T)$ without loose coupling at the site. This same conclusion was seen to hold for E_1' centers, but for E_2' it is clearly unambiguous.

Furthermore, the effect of the neglected strain of the phonons near the characteristic frequency may explain the slight excess of the data points in the neighborhood of 45°K over the solid curve. The curve was calculated from Eq. (17) according to the stated approximation and fitted to the observations at 80°K. The excess around 45°K is about 25% and apparently persists between 20 and 60°K. The excess cannot be accounted for by the fourth term in (17); this term, disregarded in our numerical fit, would contribute about 3% to the calculated curve at $T=45°K$. A similar effect could have been found in E_1' if the T^3 term had been fitted at a temperature well above the characteristic 140°K temperature.

VII. SUMMARY WITH RESPECT TO E' CENTERS

The spin-lattice relaxation of E_1' and E_2' centers in synthetic quartz has been measured at 3000 Oe with sufficient accuracy and over a sufficient range of temperature and samples to indicate several specific features of the electronic configuration for each type of center. The models proposed here and in the companion paper are certainly consistent with the presence of low characteristic frequencies of local distortion around each center; the assignment of one of the observed frequencies to the presence of a proton is apparently unambiguous. Refinement of details is expected after similar relaxation measurements at higher magnetic fields and in other types of quartz samples.

Raman relaxation is found to represent another strong similarity in electron configuration between E_1' and E_2' centers.

VIII. SUMMARY WITH RESPECT TO RAMAN RELAXATION AT DEFECT SITES

Raman relaxation at defect sites characterized by a low frequency of local distortion is shown to have a lower temperature dependence than the corresponding

Raman relaxation in a perfect lattice. An explicit expression is derived under the assumption of harmonic response of the local distortion at the defect site. The close fit to the data for the E' centers, within about 20% over six orders of magnitude variation in T_1, supports the validity of this method of calculation of Raman relaxation processes of defect sites. Such defect relaxation may be quite common.

APPENDIX. LOCAL STRAIN AT A DEFECT SITE ASSUMING HARMONIC RESPONSE AND VELOCITY DAMPING

The local strain at a defect site was discussed in Sec. III but damping was neglected. Damping of such motion whose frequency is within the acoustic branch of the crystal has previously been assumed to be very severe, whereas it actually may be quite moderate. In either case the following calculation applies to the extent that velocity damping is an adequate description.

The quantity of interest (Sec. III) is the modulus of the local strain per phonon at the defect site as a function of phonon frequency for each of several conditions of damping. For convenience, velocity-damping is introduced into the calculation of the forced harmonic oscillator response giving the equation of motion

$$d^2v/dt^2=-\lambda\omega_i(dv/dt)-\omega_i^2(v-u) \qquad \text{(A1)}$$

instead of Eq. (10). For the incident phonon $u=ae^{i\omega t}$ as before, the response of the defect is taken as $v=be^{i(\omega t+\phi)}$. Then the local strain is given by

$$\epsilon'=(v-u)/a_0=(a/a_0)Re^{i(\omega t+\beta)} \qquad \text{(A2)}$$

and the modulus $(a/a_0)R$ is substituted into the Hamiltonian, such as Eq. (1). The solution of Eq. (A1) gives the reduced strain modulus R as

$$R=\frac{\{[(1-f^2)-(1-f^2)^2-\lambda^2f^2]^2+\lambda^2f^2\}^{1/2}}{(1-f^2)^2+\lambda^2f^2}, \qquad \text{(A3)}$$

where f is the reduced phonon frequency, ω/ω_i. Equation (A3) holds for all values of the damping factor λ; R is plotted in Fig. 5 for $\lambda=1$ and $\lambda=\frac{1}{3}$. The value of $\lambda=\frac{1}{3}$ corresponds to the lifetime estimated by Brout and Visscher[27] for $\omega_i=\omega_D/5$ in a Bravais lattice.

The applicability of Eq. (A3) to a real defect is open to question on the basis that the actual damping of the excess local strain may not be velocity damping. Therefore, one might expect the response for the higher phonon frequencies to be less than that indicated by Eq. (A3) and the approximation of Eqs. (12) and (13) might not underestimate the strain modulus over the frequency range.

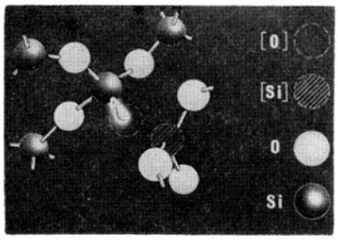

FIG. 1. Proposed structural model for the E_2' center in crystalline quartz. The crystal ball model is shown as viewed about 30° from a [10·0] axis. Regular lattice positions of the silicon and oxygen ions are indicated even though static relaxation around the defect is expected. The locations of the interstitial(s) are not shown.

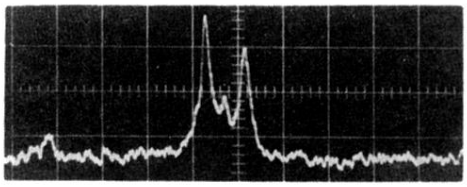

FIG. 2. Resonance absorption by E_2' centers of 9 Gc/sec radiation with the applied field H parallel to the [00·1] axis of sample *CQ*-10 at 73°K. The photograph of the oscilloscope screen shows the three resonance lines for silicon 28 centers with the vertical scale linear in microwave emf and the horizontal scale, linear in magnetic field. The separation of the two large peaks is about 0.4 Oe.

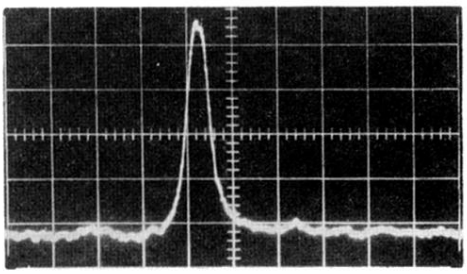

FIG. 3. Resonance absorption of E_1' centers of 9 Gc/sec radiation with the applied field H parallel to the [00·1] axis of sample *GQ*-9 at 4.2°K. The photograph of the oscilloscope screen shows the resonance line for silicon 28 centers with the vertical scale linear in microwave emf and the horizontal scale, linear in magnetic field. The full line width as seen is less than 0.1 Oe.

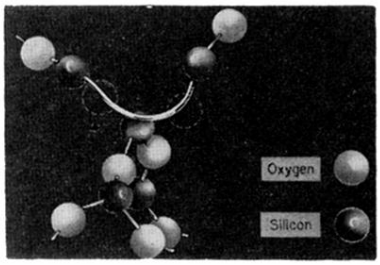

FIG. 4. Proposed structural model for the E_1' center in crystalline quartz. The crystal-ball model is shown as viewed along [10·0]. Regular lattice positions of the silicon and oxygen ions are indicated even though static relaxation of the lattice around the defect is expected. The location(s) of the interstitial is not shown.

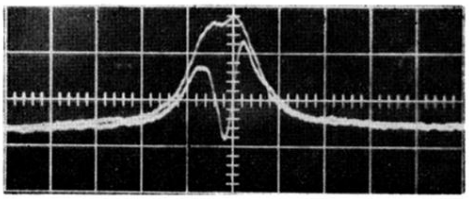

FIG. 7. Holes in the resonance line of E_1' centers in *GQ*-9 at 27.3°K. The delay times for the two traces are 0.10 and 1.70 sec. The complete line was observed to have $T_1=0.44$ sec at this temperature.

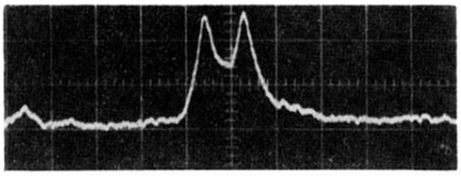

FIG. 9. Resonance absorption of E_2' centers in *CQ*-10 at 4.2°K. Conditions are identical to those for Fig. 2 except for the temperature. The separate resonances are considerably broader.